

K-band EPR of photoinduced midgap states in an M - X chain complex $[\text{Pt}(\text{en})_2][\text{Pt}(\text{en})_2\text{Cl}_2](\text{ClO}_4)_4$, (en) = ethylenediamine

Noritaka Kuroda, Motoki Ito,* and Yuichiro Nishina

Institute for Materials Research, Tohoku University, Katahira 2-1-1, Aoba-ku, Sendai 980, Japan

Asako Kawamori, Yoshio Kodera, and Takaya Matsukawa

Department of Physics, Faculty of Science, Kwansei Gakuin University, Nishinomiya 662, Japan

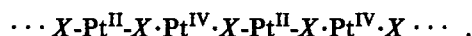
(Received 9 February 1993)

The K-band electron paramagnetic resonance due to the photoinduced midgap state has been measured in an M - X chain complex $[\text{Pt}(\text{en})_2][\text{Pt}(\text{en})_2\text{Cl}_2](\text{ClO}_4)_4$, (en) = ethylenediamine, at 77 K. The angular variations of the spectral line shape and the intensity show that the photoinduced unpaired electron is localized on the segment Pt-Cl-Pt of the M - X chain bonds. The p_σ orbit of the intervening Cl^- ion is found to share 30–40% of the density of the unpaired electron, based on the following hyperfine constants of the constituent ^{195}Pt and $^{35,37}\text{Cl}$ nuclei: $A_{\parallel}^{\text{Pt}} = 378 \times 10^{-4} \text{ cm}^{-1}$ and $A_{\parallel}^{\text{Cl}} = 55 \times 10^{-4} \text{ cm}^{-1}$ for the quantization direction parallel to the chain axis; $A_{\perp}^{\text{Pt}} = 375 \times 10^{-4} \text{ cm}^{-1}$ and $A_{\perp}^{\text{Cl}} < 5 \times 10^{-4} \text{ cm}^{-1}$ for the direction perpendicular to the chain axis. The present result supports the notion that the photoinduced state is the spin soliton of two-site-type propagating along the M - X chain bonds. The possibility of the polaron is clearly excluded.

I. INTRODUCTION

In one-dimensional Peierls systems, the electronic excitations are forced to localize spatially by the electron-lattice coupling. The self-localized excitations may have a variety of forms, i.e., self-trapped exciton, polaron, soliton, and their binary forms. The properties of these excitations, particularly in conjugate polymers such as *trans*-polyacetylene, have been the subject of extensive studies. Since the presence of a midgap state was proved spectroscopically also in an M - X chain complex of platinum,¹ the self-localized excitations in the M - X chain complexes have attracted much attention to date.

The M - X chain complexes of platinum are the typical substances which belong to the category of the Peierls semiconductors. These platinum complexes are represented as $(\text{Pt}L_2)(\text{Pt}L_2X_2)Y$, where L is the ligand molecule coordinated with each Pt ion, X is the halogen ion bridging the Pt ions, and Y denotes the counterion(s). The linear M - X chain bondings $\cdots \text{Pt}-X-\text{Pt}-X-\text{Pt}-X \cdots$ are supported parallel to each other by the hydrogen-bond network joining L and Y . The mean valence of a Pt ion in this chain is 3. However, even under the ambient conditions, the electron-lattice coupling causes the halogen ions to displace periodically from the midpoint between adjacent Pt ions to form a charge-density-wave state denoted as follows:



As a result, an energy gap opens between the $5d_z^2$ states of Pt^{II} and Pt^{IV} . The value of the energy gap is 1–3 eV depending on the components of the substance.²

In several substances of the M - X complexes of platinum, if the crystal is irradiated by blue or ultraviolet light at a low temperature, a few optical-absorption bands are induced in a spectral region deep inside the fundamental energy gap. In particular, in the complex comprising L = ethylenediamine, X = Cl, and Y = $(\text{ClO}_4)_4$ (hereafter this substance is called Pt·Cl for convenience), a pair of photoinduced absorption bands appear around 1.6 and 2.0 eV,³ of which the former energy is equal to half of the energy gap of ~ 3 eV.⁴ At the same time, the electron paramagnetic resonance (EPR) is also induced.⁵ Both the midgap absorption and EPR persist as long as the crystal is kept at a temperature below about 200 K. These facts suggest that a certain long-lived electronic state is created from photoexcited electron-hole pairs through an electron-transferring relaxation process.⁶ This state is expected to be strongly localized because of a strong electron-lattice coupling that is evidenced by the large energy gap. The Peierls-Hubbard model predicts that the electronic correlation plays an important role in characterizing such a self-localized state.⁷

A weak spectrum that is identical to the photoinduced one can be observed in either of the optical-absorption^{1,6}

and EPR (Ref. 8) spectra of the pristine unirradiated crystals of Pt·Cl. The intensities of the spectra suggest that one Pt ion per several thousand to ten thousand Pt ions has an anomalous valence.^{1,8} From the measurement of EPR in pristine crystals, Kawamori, Aoki, and Yamashita⁸ have proposed that the local anomalies in the form of Pt^{2.5}-H-Pt^{2.5} are introduced in the chains during the crystal growth. Subsequently, Kuroda *et al.*⁹ have claimed, on the basis of the angle and temperature dependences of the photoinduced EPR spectrum, that mobile Pt dimers in the form of Pt^{2.5}-Cl⁻-Pt^{2.5} and Pt^{3.5}-Cl⁻-Pt^{3.5} are induced. The former proposal is related to a usual paramagnetic defect, whereas the latter one means a self-localized excitation, that is, the spin soliton state. On the other hand, Suzuki and Nasu¹⁰ and Arrington *et al.*¹¹ have proposed a polaron model of the two-site type in such the form as Cl-Pt^{2.5}-Cl-Pt⁴-Cl-Pt^{2.5}-Cl. There has been, however, little decisive evidence for any of these conflicting proposals.

In the present paper, we report experimental data of the photoinduced EPR in Pt·Cl. We observe the EPR with the *K*-band microwave (wavelength ≈ 1.2 cm) instead of the standard *X*-band microwave (wavelength ≈ 3 cm). This measurement enables us to separate the possible Zeeman splitting and the hyperfine splitting from the complicated spectrum observed when the direction of the applied magnetic field is inclined from the normal to the *M-X* chain bonds. On the basis of the data obtained from this measurement, we reexamine the local structure of the EPR center. The result will be discussed in relation to the nature of the photoinduced self-localized state in Pt·Cl.

II. EXPERIMENT

The *K*-band EPR spectrum is observed by using a homemade microwave bridge coupled with a cylindrical TE₀₁₁ cavity which is tuned to a microwave frequency of 24.58 GHz. The magnetic field is generated by a Varian E109 electromagnet. The field is modulated with a frequency of 100 kHz, and the resonance absorption signal is detected with a Varian 109 lock-in system.

The experiment is conducted with single crystals grown in the shape of a rectangular platelet. The characteristic dichroism is utilized to know which of these edges is parallel to the direction of the *M-X* chain axis. A single crystal in size of about $2 \times 4 \times 0.5$ mm³ is put in a Suprasil quartz tube with an inner diameter of 3 mm. The *M-X* chain axis is oriented perpendicular to the tube axis, so that the applied magnetic-field direction can be varied from parallel to perpendicular to the *M-X* chain axis. The sample tube is immersed in liquid nitrogen and illuminated by a 150-W xenon arc lamp through a blue filter (Toshiba V-B46) and a condenser lens. Then the sample tube is transferred quickly into the cavity without a temperature raise.

III. EXPERIMENTAL RESULTS

Within the sensitivity of our instrument, no EPR signal can be detected for unirradiated crystals. The photo-

induced spectrum develops if the sample is exposed to the blue light for 5–10 min. The resonance field, the resonance pattern, and the intensity vary with the direction of the applied magnetic field. Figure 1 shows three typical spectra, i.e., the spectra observed with the field applied parallel, at an angle 37.5°, and perpendicular to the *M-X* chain axis. Since the location of the whole resonance spectrum varies widely in a field range from 0.70 to 0.95 T upon changing the field direction, the field given by $h\nu/(g_{\theta}\mu_B)$ is chosen as the origin of the abscissa for each spectrum in Fig. 1, where $h\nu$ is the photon energy of the microwave, g_{θ} is the effective *g* value for the field applied at the angle θ to the chain axis, and μ_B is the Bohr magneton; g_{θ} is given by

$$g_{\theta} = (g_{\parallel}^2 \cos^2 \theta + g_{\perp}^2 \sin^2 \theta)^{1/2}, \quad (1)$$

with $g_{\parallel} = 1.943 \pm 0.002$ and $g_{\perp} = 2.293 \pm 0.002$. Despite the fact that the microwave frequency 24.58 GHz is nearly three times the frequency of the *X*-band microwave used in the previous experiments,^{8,9,12} the observed resonance pattern is almost identical to the previous one for all directions of the applied field. Contrary to a presumption that two species of spins with appreciably different *g* parameters coexist,^{9,12} the resonance signals seem to originate from a single species of the paramagnetic state.

For $\theta = 90^\circ$, symmetric fivefold structures are observed. This pattern is unique to the hyperfine structure due to the dimerized platinum nuclei.¹³ Among several isotopes of Pt, only ¹⁹⁵Pt possesses a nonvanishing nuclear spin of $\frac{1}{2}$; its natural abundance is 33.7%. Let the total nuclear spin of a Pt dimer be I^{Pt} and its magnetic quantum number be m . Then, three nuclear states $I^{\text{Pt}} = 0, \frac{1}{2}, \text{ and } 1$ are possible. These nuclear states are quantized by the applied magnetic field into the Zeeman sublevels corresponding to $m = -1, -\frac{1}{2}, 0, \frac{1}{2}, \text{ and } 1$ with a statistical probability ratio of about 1:8:18:8:1, as shown in Fig. 2(a). Each line of this hyperfine spectrum consists of the

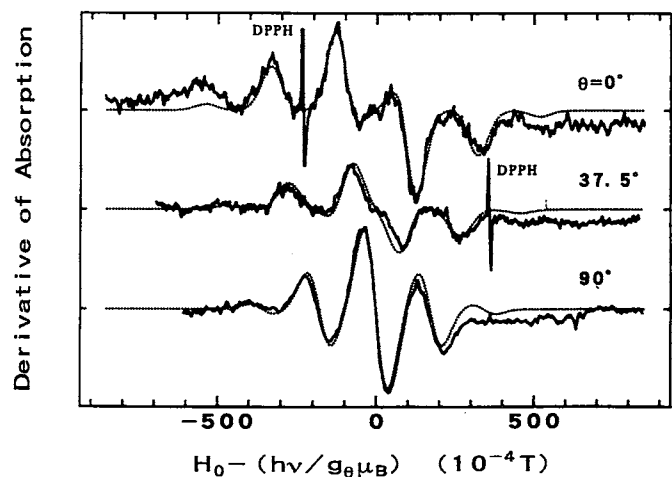


FIG. 1. Photoinduced EPR spectra in PtCl at 77 K. The microwave frequency ν is 24.58 GHz. The solid lines are the experimental spectra. The dotted lines are the theoretical spectra for the Pt dimer plus one Cl composite.

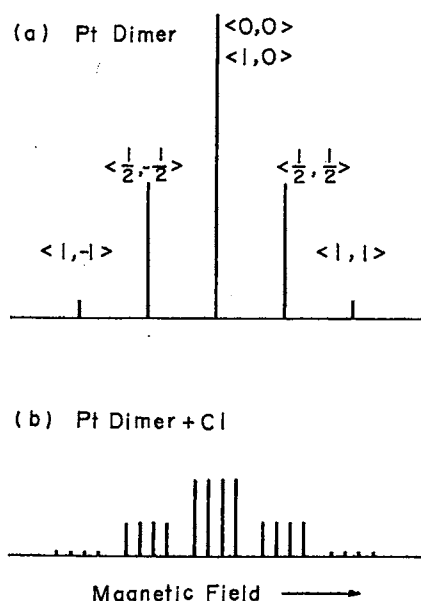


FIG. 2. First-order hyperfine structures expected for (a) the Pt dimer and (b) the Pt dimer plus one Cl composite. Each line in (a) is assigned in the representation $\langle I^{\text{Pt}}, m \rangle$.

superhyperfine components due to ^{14}N nuclei of ethylenediamines coordinated with Pt ions and to $^{35,37}\text{Cl}$ nuclei located on both sides of the Pt dimer.^{8,12}

If θ deviates from 90° , the whole spectrum seems to split twofold further in almost the same way as observed with the X-band microwave. An assignment of the origin of this splitting is the hyperfine interaction with a proton which has been substituted for the Cl^- ion intervening between the dimerized Pt ions.⁸ However, the observed variation of the resonance pattern with θ , particularly around $\theta=0^\circ$, is difficult to simulate in terms of the twofold splitting regardless of the origin. In the following, we show that this splitting is not twofold but fourfold, due to a single nucleus possessing a spin of $\frac{3}{2}$, i.e., the $^{35,37}\text{Cl}$ nucleus itself.

Figure 2(b) illustrates the hyperfine structures expected for a composite of the Pt dimer and a Cl^- ion. The spin Hamiltonian for such a composite is written as

$$H = \mu_B \mathbf{S} \cdot \vec{g} \cdot \mathbf{H}_0 + \mathbf{S} \cdot \vec{A}^{\text{Pt}} \cdot \mathbf{I}^{\text{Pt}} + \mathbf{S} \cdot \vec{A}^{\text{Cl}} \cdot \mathbf{I}^{\text{Cl}}, \quad (2)$$

where \mathbf{S} is the electron spin of $S = \frac{1}{2}$, \vec{g} is its g tensor given by Eq. (1), \mathbf{H}_0 is the applied magnetic field, \vec{A}^{Pt} is the hyperfine tensor of a Pt dimer, \mathbf{I}^{Pt} is the total nuclear spin of a dimer, \vec{A}^{Cl} is the hyperfine tensor of the $^{35,37}\text{Cl}$ nucleus, and \mathbf{I}^{Cl} is the spin of the $^{35,37}\text{Cl}$ nucleus. The resonance pattern can be easily calculated if the principal values of \vec{A}^{Pt} and \vec{A}^{Cl} and the line shape of each hyperfine line are given. Since each line consists of overlapped superhyperfine components as already mentioned, its line shape can be represented by a Gaussian function. In the present analysis, we choose the Gaussian width 54×10^{-4} T and assume for simplicity that the width is independent of the field direction. In addition, we neglect a small difference expected for \vec{A}^{Cl} between ^{35}Cl and ^{37}Cl nuclei. In Fig. 1, the theoretical resonance patterns are drawn in comparison to the experimental spectra. The

values of the hyperfine constants used for the calculation are listed in Table I. The calculated spectra reproduce the experimental ones for all directions of the applied field very well. Note that for $\theta=0^\circ$ the dominant features around the origin of the field, which are associated with the $m=0$ states of Pt nuclei, consist of a pair of isolated positive and negative peaks. We see that this pattern comes uniquely from the fourfold, flat and equidistant, splitting due to the $^{35,37}\text{Cl}$ nucleus.

The intensities of the calculated curves shown in Fig. 1 are adjusted so as to match the instrumental gain for each spectrum. It may be worth noting here that the intensity of the resonance absorption depends significantly on θ . Figure 3 shows a plot of the experimental peak-to-peak intensity I_{pp} of the central line as a function of θ . The value of I_{pp} decreases slightly with increasing θ from 0° to 30° and then turns to increase rapidly as θ increases further. This is consistent with our picture of the photoinduced state. The calculated θ dependence of I_{pp} is compared to the experimental data in Fig. 3. The calculated curve reproduces the behavior of I_{pp} well. In the present calculation, the Gaussian width is assumed constant. However, it should also depend on θ , giving rise to an additional θ dependence of I_{pp} . It is mainly for this reason that a systematic discrepancy occurs between the experimental data and the calculated curve.

As seen from Table I, the hyperfine tensor \vec{A}^{Cl} of the $^{35,37}\text{Cl}$ nucleus is highly anisotropic. This anisotropy comes from the p orbit. Suppose the p orbit is directed toward the chain axis. Neglecting a small contribution from the direct dipole-dipole interaction, the principal values $A_{\parallel}^{\text{Cl}}$ and A_{\perp}^{Cl} are given by¹⁴

$$A_{\parallel}^{\text{Cl}} = a_s + 2a_p, \quad (3)$$

$$A_{\perp}^{\text{Cl}} = a_s - a_p, \quad (4)$$

where the subscripts \parallel and \perp refer to the directions relative to the M - X chain axis, a_s is the contribution from the s orbit and/or the core polarization, and a_p is the contribution from the p orbit. We have $A_{\perp}^{\text{Cl}} \approx 0$, and thus Eq. (4) gives $a_s \approx a_p$. It follows from Eq. (3) that $A_{\parallel}^{\text{Cl}} \approx 3a_p$. Using the experimental value $A_{\parallel}^{\text{Cl}} = 55 \times 10^{-4} \text{ cm}^{-1}$, we obtain $a_p \approx 18 \times 10^{-4} \text{ cm}^{-1}$. If a single unpaired electron occupies the $3p_z$ orbit of a free Cl atom, a_p is expected to be $46 \times 10^{-4} \text{ cm}^{-1}$ and $39 \times 10^{-4} \text{ cm}^{-1}$ for ^{35}Cl (abundance = 75.5%) and ^{37}Cl (abundance = 24.5%) nuclei, respectively.¹⁵ In the present case, an average over the splittings due to these Cl isotopes is observed. The experimental value of a_p suggests that the unpaired electron spends nearly 40% of its time on the p orbit of the Cl^- ion. There is no doubt that this p orbit makes a σ bonding with the $5d_z^2$ orbitals of dimerized Pt ions.

TABLE I. The principal values of the hyperfine tensors \vec{A}^{Pt} and \vec{A}^{Cl} of ^{195}Pt and $^{35,37}\text{Cl}$ nuclei, respectively.

Direction	$A^{\text{Pt}} (10^{-4} \text{ cm}^{-1})$	$A^{\text{Cl}} (10^{-4} \text{ cm}^{-1})$
\parallel chain	378 ± 2	55 ± 2
\perp chain	375 ± 2	< 5

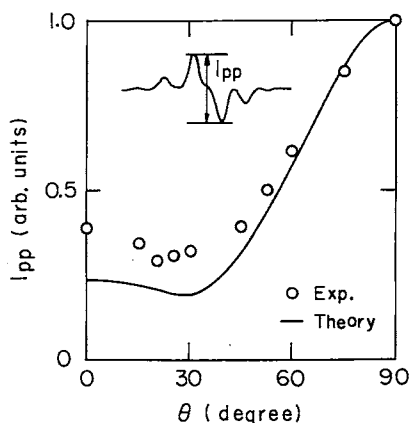


FIG. 3. Angle dependence of the peak-to-peak intensity of the central line; θ is the angle between the applied field and the M - X chain axis. The open circles are the experimental values and the solid line is the theoretical curve for the Pt dimer plus one Cl composite.

Similar Pt dimers are produced in K_2PtCl_4 by γ irradiation.¹³ In this substance, Pt ions on the nearest-neighbor sites are directly dimerized. The hyperfine constants are 444×10^{-4} and $618 \times 10^{-4} \text{ cm}^{-1}$ for the quantization directions parallel and perpendicular to the dimerization axis, respectively. We see from Table I that the value of $A_{\parallel}^{Pt} + 2A_{\perp}^{Pt}$ in Pt-Cl is reduced to 67% of the corresponding quantity in K_2PtCl_4 . This fact also suggests that the p_{σ} bonding due to the Cl^{-} ion is formed in Pt-Cl by transferring more than 30% of the unpaired electron from the Pt $5d_z^2$ state.

IV. FORM OF THE PHOTOINDUCED STATE

It is now evident from the above analysis that, apart from the nuclei contributing to the superhyperfine splitting which gives the width of each hyperfine line, two Pt ions and one Cl^{-} ion comprise the photoinduced paramagnetic state. The polaron model proposed by Suzuki and Nasu¹⁰ and Arrington *et al.*¹¹ involves four nearly equivalent Cl nuclei, as cited in Sec. I. Clearly, the present result excludes the polaron model.

The Cl^{-} ion comprising the photoinduced composite state is bonded to the Pt ions by the p orbit directed toward the chain axis. It is natural to associate this composite with a segment of the M - X chain bonds. In view of another fact that the two constituent Pt ions are dimerized, i.e., the Pt ions are magnetically almost identical to one another, the possible structures are only $\cdots Pt^{2.5}-Cl^{-}-Pt^{2.5} \cdots$ and $\cdots Pt^{3.5}-Cl^{-}-Pt^{3.5} \cdots$. As shown later, the Cl^{-} ion is expected to sit at the middle between the two Pt ions in the thermal equilibrium. In the present substance, the valence and conduction bands are formed by the antibonding orbitals between Pt $5d_z^2$ and Cl $3p_z$ or $3s$ states.¹⁶ Figure 4 illustrates the molecular-orbital energy-level schemes in this situation. Note that the $3p_z$ and $3s$ orbits of a Cl^{-} ion have the local states split into the ungerade and gerade levels, respectively. Since the $3s$ state lies much lower in energy than the $3p_z$ state in the free Cl^{-} ion, the gerade level

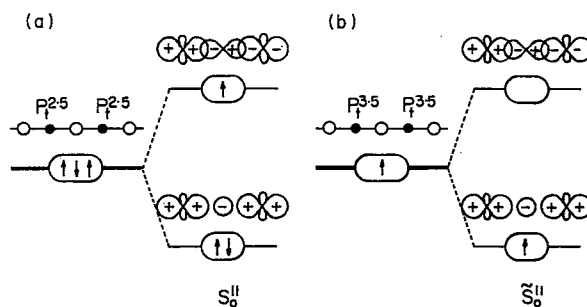


FIG. 4. Molecular-orbital schemes of the energy-level splitting in (a) $Pt^{2.5}-Cl-Pt^{2.5}$ and (b) $Pt^{3.5}-Cl-Pt^{3.5}$.

would lie lower than the ungerade level. Based on our experimental result, the observed unpaired electron is expected to be accommodated in the ungerade level of $\cdots Pt^{2.5}-Cl^{-}-Pt^{2.5} \cdots$. We note that the obtained energy-level scheme corresponds to what has been conceived by Kawamori, Aoki, and Yamashita⁸ concerning the defect $Pt^{2.5}-H-Pt^{2.5}$.

The above consequence gives us insight into the nature of the photoinduced state. In the M - X chain complexes, the electron-lattice coupling for a pair of a Pt ion and the adjacent Cl^{-} ion is given well by the product ξnu ,¹⁷ where n is the number of the valence electrons in the $5d_z^2$ orbit of the Pt ion, u is the displacement of the Cl^{-} ion toward the Pt ion, and ξ (>0) is the coupling coefficient. The competition of the energy gain due to the electron-lattice coupling with the elastic energy which is proportional to u^2 determines the equilibrium value of u principally. The electron-lattice coupling is so strong that $|u|$ amounts to 0.4 \AA in the ground state as shown in Fig. 5. Therefore, the Cl^{-} ion of $\cdots Pt^{2.5}-Cl^{-}-Pt^{2.5} \cdots$ must be located at the middle between the two Pt ions. Similarly, on both sides of the paramagnetic segment, the displace-

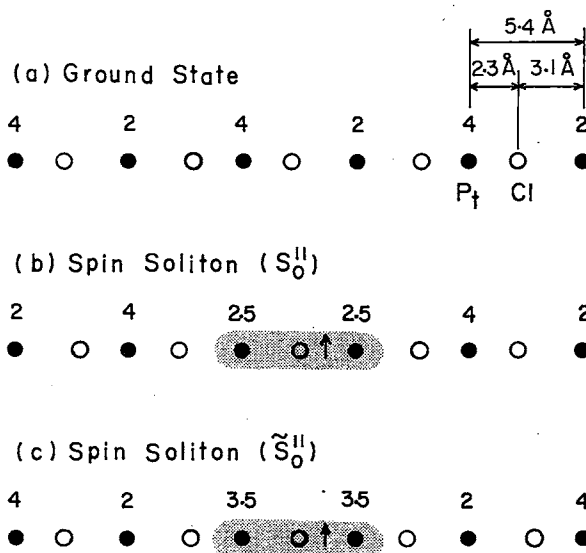


FIG. 5. Valence structures of (a) the ground state, (b) the spin soliton of the two-site type S_0^{II} , and (c) its conjugate state \tilde{S}_0^{II} . Numerals are the ideal valencies of Pt ions. Vertical arrows denote unpaired spins spreading over the shaded area.

ments of Cl^- ions and thus the valences of Pt ions must be centrosymmetric as illustrated in Fig. 5. Note that the resulting phases of u and the charge-density wave of Pt ions are reversed on either side. This state is the two-site-type spin soliton S_0^{II} , which has been treated theoretically by Kuroda, Kataoka, and Nishina.⁷

As seen from Fig. 5, the state $\cdots \text{Pt}^{3.5}\text{-Cl}^-\text{-Pt}^{3.5}\cdots$ should also be a spin soliton of two-site type: It is referred to as \tilde{S}_0^{II} in Ref. 7. S_0^{II} and \tilde{S}_0^{II} transform themselves into one another upon every translation along the chain by a lattice constant. (See Fig. 16 of Ref. 7.) The present experimental result strongly suggests that only the pairs of S_0^{II} and its antiphase form are stable practically. However, within the framework of an extended Peierls-Hubbard model,^{10,17} S_0^{II} and \tilde{S}_0^{II} have the same formation energies, so that they may coexist. This is a consequence of the assumption that the electron transfer between adjacent Pt ions is independent of the orbital states of the intervening Cl^- ion. The present experimental result raises a question about the validity of such an assumption.

Finally, we would like to mention the origin of the superhyperfine splitting. It is now apparent that the explanation by Arrington *et al.*¹¹ in terms of the polaron model is misleading. In previous work in which some of the present authors contributed,¹² the superhyperfine structures observed for $\theta \approx 90^\circ$ below 50 K have been assigned to two ^{35,37}Cl nuclei neighboring the unpaired electron site of \tilde{S}_0^{II} and eight ¹⁴N nuclei of ethylenediamines coordinated with Pt ions of \tilde{S}_0^{II} and S_0^{II} . A parallel argument is valid even if only the S_0^{II} state is present in the crystal. The point suggested by the angle dependence of the fine structures^{8,9,12} and an isotope effect¹¹ is that ^{35,37}Cl nuclei neighboring S_0^{II} and ¹⁴N nuclei of ethylenediamines interact with the unpaired electron concurrently. In such cases, since the energy-level scheme of the unpaired spin is very complicated generally, the appearance of clear fine structures is rather accidental. Presumably, a small value of A_{I}^{Cl} of the central Cl nu-

cleus helps the appearance of the fine structures for $\theta \approx 90^\circ$.

V. SUMMARY

We have presented the results of the measurement of the K-band EPR in optically irradiated crystals of an *M-X* chain complex $[\text{Pt}(\text{en})_2][\text{Pt}(\text{en})_2\text{Cl}_2](\text{ClO}_4)_4$. On the basis of the data obtained from this measurement, the local structure of the photoinduced EPR center has been reexamined. It has turned out that the overall EPR signals can be explained consistently by modeling the photoinduced center as a composite of dimerized Pt nuclei and one Cl nucleus. The hyperfine tensors of the constituent Pt and Cl nuclei show that these nuclei are bonded together by the Cl $3p$ orbit which is directed toward the chain axis sharing 30–40% of the density of the unpaired electron. This finding proves that the composite is a segment Pt-Cl-Pt of the linear chain bonds, being involved with no imperfections of the lattice. The segment bears three valence electrons, of which the unpaired electron is accommodated in the antibonding molecular orbital consisting of Pt $5d_z^2$ and Cl $3p_z$ orbitals. The paramagnetic state that may be stable in such a form under the influence of a strong electron-lattice coupling is attributable to the spin soliton state S_0^{II} of two-site type.

Another two-site-type spin soliton state \tilde{S}_0^{II} which has the same formation energy as S_0^{II} in an extended Peierls-Hubbard model cannot be detected within our experimental sensitivity. The state \tilde{S}_0^{II} is supposed to bear a single valence electron in the molecular orbital of Pt $5d_z^2$ and Cl $3s$. The absence of \tilde{S}_0^{II} suggests that the orbits of Cl^- ions should be taken explicitly into account to understand the nature of the self-localized states in the present group of substances.

ACKNOWLEDGMENT

One of the authors (N.K.) is grateful to Dr. M. Kataoka for illuminating discussions.

*Present address: Kyocera Co., Ltd., Yohkaichi 527, Japan.

¹N. Kuroda, M. Sakai, Y. Nishina, M. Tanaka, and S. Kurita, *Phys. Rev. Lett.* **58**, 2122 (1987).

²H. Okamoto, T. Mitani, K. Toriumi, and M. Yamashita, *Mater. Sci. Eng. B* **13**, L9 (1992).

³S. Kurita, M. Haruki, and K. Miyagawa, *J. Phys. Soc. Jpn.* **57**, 1798 (1988).

⁴Y. Wada and M. Yamashita, *Phys. Rev. B* **42**, 7398 (1990).

⁵S. Kurita and M. Haruki, *Synth. Metals* **29**, F129 (1989).

⁶M. Sakai, N. Kuroda, and Y. Nishina, *Phys. Rev. B* **40**, 3066 (1989).

⁷N. Kuroda, M. Kataoka, and Y. Nishina, *Phys. Rev. B* **44**, 13 260 (1991).

⁸A. Kawamori, R. Aoki, and M. Yamashita, *J. Phys. C* **18**, 5487 (1985).

⁹N. Kuroda, M. Sakai, M. Suezawa, Y. Nishina, and K. Sumino, *J. Phys. Soc. Jpn.* **59**, 3049 (1990).

¹⁰M. Suzuki and K. Nasu, *Phys. Rev. B* **45**, 1605 (1992).

¹¹C. A. Arrington, C. J. Unkefer, R. J. Donohoe, S. C. Hockett, S. Kurita, and B. I. Swanson, *Solid State Commun.* **84**, 979 (1992).

¹²M. Sakai, N. Kuroda, M. Suezawa, Y. Nishina, K. Sumino, and M. Yamashita, *J. Phys. Soc. Jpn.* **61**, 1326 (1992).

¹³T. Krigas and M. T. Rogers, *J. Chem. Phys.* **55**, 3035 (1971).

¹⁴J. W. Orton, *Electron Paramagnetic Resonance: An Introduction to Transition Group Ions in Crystals* (Iliffe, London, 1968), Chap. 8.

¹⁵J. E. Wertz and J. R. Bolton, *Electron Spin Resonance: Elemental Theory and Practical Applications* (McGraw-Hill, New York, 1972).

¹⁶M. H. Whangbo and M. J. Foshee, *Inorg. Chem.* **20**, 113 (1980).

¹⁷D. Baeriswyl and A. R. Bishop, *J. Phys. C* **21**, 339 (1988).